Vietnam Journal of Earth Sciences, 42(4), 363–383, Doi: 10.15625/0866-7187/0/0/15410

(VAST)

Vietnam Academy of Science and Technology

Vietnam Journal of Earth Sciences

http://www.vjs.ac.vn/index.php/jse

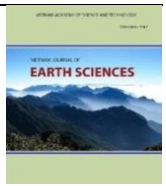

Assessment of shoreline changes for setback zone establishment from Son Tra (Da Nang city) to Cua Dai (Hoi An city), Vietnam

Ngo Van Liem[1*], Dang Van Bao[1], Dang Kinh Bac[1], Ngo Chi Cuong[1], Pham Thi Phuong Nga[1], Benjamin Burkhard[2, 3], Giap Thi Kim Chi[4]

[1]*VNU University of Science, Vietnam National University, Hanoi, Vietnam*
[2]*Institute of Physical Geography and Landscape Ecology, Leibniz Universität Hannover, Schneiderberg 50, 30167 Hannover, Germany*
[3]*Leibniz Centre for Agricultural Landscape Research ZALF, Eberswalder Straße 84, 15374 Müncheberg, Germany*
[4]*Institute of Geological Sciences, VAST, Hanoi, Vietnam*

Received 8 June 2020; Received in revised form 10 August 2020; Accepted 7 October 2020

ABSTRACT

The most important function of the coastal setback is to minimize damage due to coastal erosion, climate change response, and sea-level rise. There are many directions and methods of researching and assessing coastal changes and coastal erosion. This study presents the results of the shoreline changes in the area from Son Tra (Da Nang City) to Cua Dai (Hoi An City), Central Vietnam based on remote sensing data from 1965 to 2019. Three methods are used to include End Point Ratio (EPR), Linear Regression Rate (LRR), and Weighted Linear Regression (WLR). The results show that the EPR method is effective when calculating the rate of shoreline changes only at two different times. For more objective and reliable calculation, it is necessary to assess the shoreline changes over time. Meanwhile, the LRR method was shown to be superior because all shoreline data were taken into account during the construction of the regression line. However, when there is much shoreline data with different reliability, the WLR method proved more superior because of limited objective errors. The results show that from 1965 to 2019, the coast of the Son Tra - Cua Dai area had quite complicated fluctuations, of which the northern area (Son Tra) tended to accretion, the central area tends to be alternate between accretion and erosion, while the south area (Cua Dai) is strong to very strong erosion. The coast with sudden changes is the Cua Dai area with the shoreline change envelope (SCE) reaching 512 m. The results also allow us to divide the coast of the Son Tra - Cua Dai area into 30 segments. They are clustered into 8 groups with different levels of erosion and accretion. This is an important basis for the setback zone establishment in the study area.

Keywords: shoreline changes; coastal erosion; setback zone; linear regression; Hoi An.

©2020 Vietnam Academy of Science and Technology

1. Introduction

Shorelines are transitional places between the ocean, continental, and atmospheric environment. Since 2000s, urbanization has become a main reason for shoreline changes (Mullick et al., 2020). Coastal processes

*Corresponding author, Email: liemnv@hus.edu.vn

depend on three main groups of factors: internal factors, external factors, and human intervention (Thoai et al., 2019). Internal factors include a wide variety of processes such as near-shore currents, wave energy, tidal inundations, changes in sediment budget, etc. (Williams et al., 2018). The natural disaster, i.e., storm surge, tsunami, coastal flood, extreme rainfalls, etc. are the external factors (Thai and Tri, 2019); whereas, deforestation, coastal urban and infrastructural development, dredging, exploitations of coastal minerals, etc. are recognized as the anthropogenic factors (Kuleli et al., 2011; Mullick et al., 2020). Human interventions destabilize the shoreline by diverting the movement landward in different parts of a coast (Mullick et al., 2020). These impacts make the world's coastline complicated, leading to serious social and environmental consequences, especially with coastal erosion.

Landward movement of the shoreline creates socio-economic problems with residents (Mullick et al., 2020). At the same time, significant economic losses from the tourism industry, ecological damage, and societal problems such as property loss are also intensified with displaced people (Aiello et al., 2013). Coastal erosion has become a major environmental problem and crisis in the coastal region throughout the world (Mullick et al., 2020). The global shoreline is continuously eroded from 0.01-10 m/year, whereas the alluvial deltas experience as an accumulated region (Pilkey and Hume, 2001). This issue has been attended by scientific communities in last few decades (Gupta et al., 2015; Moussaid et al., 2015; Natesan et al., 2015; Aouiche et al., 2016; Samanta and Paul, 2016; Hakkou et al., 2018; Mullick et al., 2020). Therefore, monitoring of shoreline change trends (spatially and temporally) is necessary to support coastal zone management plan, as well as to devise measures to prevent or minimize the effects of shoreline movement (Mullick et al., 2020).

Over the past few decades, Vietnam's coastline has been strongly transformed, especially coastal erosion and accretion of sand beaches in estuaries, which have been increasingly expanded both in scale and intensity. Coastal erosion has become common in many sections of Vietnam's coastline that were previously accumulated (Phai, 2013). Despite no human damage, coastal erosion has caused many property losses and adversely affecting the socio-economic development of coastal provinces, such as the Quang Nam - Da Nang area, especially the section from Son Tra to Cua Dai region. In order to minimize damage due to coastal erosion, a setback zone is one of the best tools for coastal management (VNA, 2015). In which, the assessment of the rate of shoreline change is one of three important contents to decide a setback zone (MONRE, 2016). This study presents the latest results of shoreline changes using different open-source remote sensing resources and the most modern methods available in calculating shoreline changes. The area from Son Tra (Da Nang city) to Cua Dai (Hoi An city, Quang Nam province) was selected for a pilot study. This area has been subjected to strong impacts of both natural and human activities (Son and Anh, 2019) and caused complicated coastal changes in recent years (Cham, 2020).

2. Regional setting

The study area is approximately 33 km long, extending from the southern part of the Son Tra Peninsula (Da Nang City) to Cua Dai (Hoi An City, Quang Nam Province),

Vietnam (Fig. 1). In terms of tectonic structure, this area is located in the relative subsidence area (Hai, 2017). In geology and geomorphology, the coast of this area is sandy coast landforms, generated mainly by Quaternary sediments with late Pleistocene to Holocene age. Coastal plains from Son Tra to Cua Dai can be classified into two types according to the differences in morphology, origin, and formation history. A sand-dune plain is generated in the north (Son Tra - Non Nuoc area), and a delta plain is in the south (Non Nuoc - Cua Dai area). Rivers in the area flow from the high mountains in the eastern slopes of the Truong Son mountain range, with peaks of 1500-2000 m high, quickly lowered to contiguous with the hills and down the plains. Therefore, all rivers in the region are characterized by short and sloping. The Son Tra - Cua Dai coastal area has a high temperature (around 25°C to 26°C) and little change during the year. Based on the temperature changes of the year, this area can be divided into two distinct seasons, the winter is from December to April and the summer is from May to November. The average annual rainfall is high (about 2763 mm), but mainly concentrated in the rainy season (from September to December), accounting for 79% of the total annual rainfall, and the daily rainfall can reach from 300 to 400 mm. The characteristics of waves and currents in the neritic zone of the study area depend mainly on the monsoon regime (the northeast direction in winter and southwest direction in summer). This area is most affected by waves during the northeast monsoon period in the direction of the NE-E wave. The general trend of coastal currents is from north to south in winter and vice versa, from south to north in summer (Mau, 2012). The neritic zone of this area has an irregular semi-diurnal tide regime with the smallest amplitude of fluctuation in Vietnam (0.8-1.2 m) (Mau et al., 2014). In particular, the average tidal range in the waters of Da Nang is about 0.7 m (Lam, 2009; Tung, 2011). Although the tides in the area are not high, the tidal currents are quite strong, and it influences on the evolution of the coastal zone (Anh, 2010). According to Thuy (1995), the average rate of the sea-level rise in the Danang area is 1.198 mm/year.

3. Database and methodology

3.1. Data collection and analyzing

In addition to a fieldwork to identify the current locations of coastal erosion, the data in the study was collected and analyzed from different data sources, including 1:50.000 topographic map in 1965 founded and published by the US military (available free of charge at the University of Texas open source: http://legacy.lib.utexas.edu/maps/topo/vietnam/; Landsat satellite images of 1973, 1990 and 2001 provided by the U.S. Geological Survey (USGS - https://earthexplorer.usgs.gov/) and satellite images from 2002 to 2019 are processed online to identify corresponding shorelines using Google Earth Pro software. Information related to the data used in the study is shown in Table 1. The satellite image information was collected from the Google Earth Pro in the study area from the website: https://discover.digitalglobe.com/.

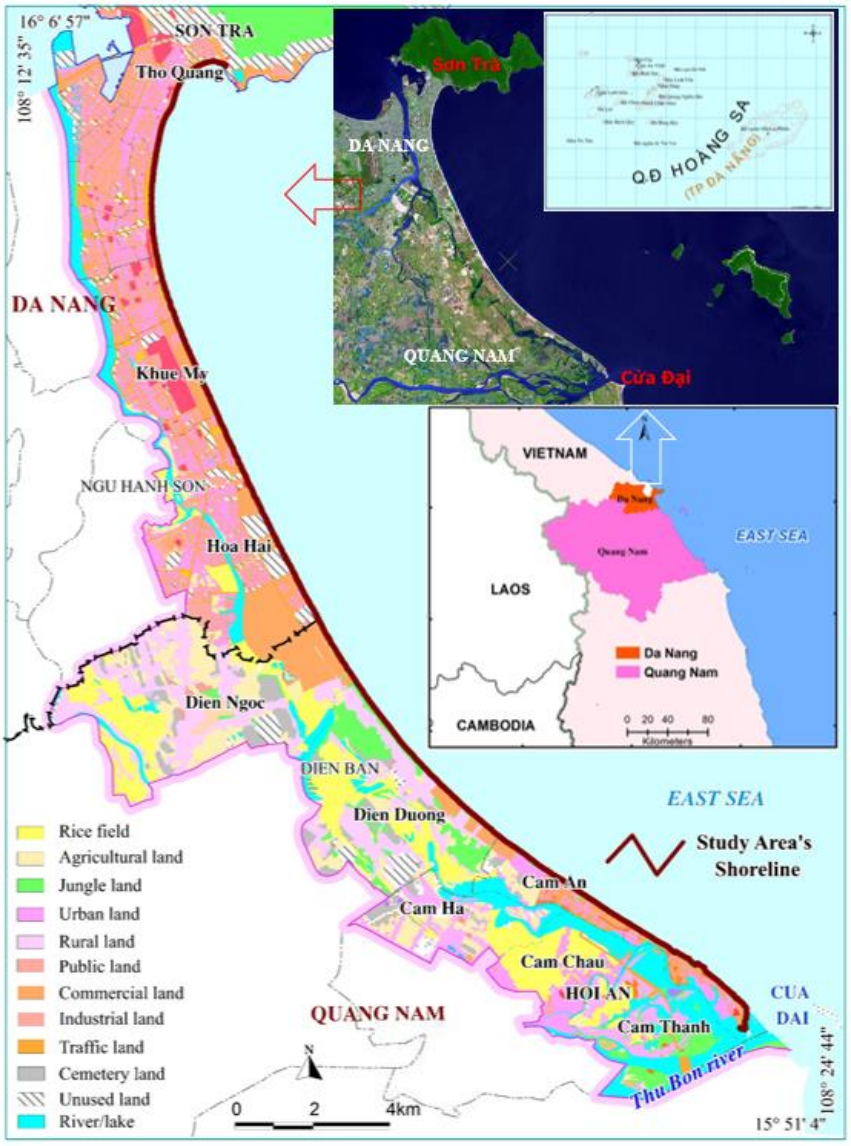

Figure 1. Location of study area

The shoreline data of 1965 was digitized manually using ArcGIS software. The shorelines of 1973, 1990 and 2001 were semi-automatically determined by the Normalized Difference Water Index (NDWI) method (Gao, 1996; McFeeters, 1996) (for satellite images in 1973) and the Modified Normalized Difference Water Index (MNDWI) (Xu, 2006) (for satellite images in 1990 and 2001). The shorelines from 2002 to 2019 after being digitized manually on Google Earth Pro software will be converted to ".kmz" format into the ".shp" format using the 2016 FME software. All data are standardized, corrected, and calculated by the use of ArcGIS software. Accordingly, the study area has identified 34 shorelines in different periods from 1965 to 2019 (see Table 1 and Fig. 6).

Table 1. Overview of data sources used in the study

No	Image ID	Time	Data type	References	Spatial resolution	Uncertainty of image interpretation (e)
1	-	1965	Topography map	Texas University	1:50.000 (30 m)	60
2	EMP133R49_ 1M19730630	30/06/1973	Landsat MSS	USGS	60 m	60
3	ETP124r49_ 5t19900824	24/08/1990	Landsat TM	USGS	30 m	60
4	ELP124R049_ 7T20010323	23/03/2001	Landsat ETM	USGS	30 m	60
5	1010010000553800	21/04/2002	QuickBird 02	Google Earth	2.4 m	7.2
6	1010010003613A00	10/11/2004	QuickBird 02	Google Earth	2.4 m	7.2
7	1010010009A3E000	20/05/2009	QuickBird 02	Google Earth	2.4 m	7.2
8	1050410001F50D00	03/02/2010	GeoEye-1	Google Earth	1.84 m	5.52
9	103001000B3EEB00	07/06/2011	Worldview 2	Google Earth	1.84 m	5.52
10	103001000F996E00	18/11/2011	Worldview 2	Google Earth	1.84 m	5.52
11	103001001274E600	10/04/2012	Worldview 2	Google Earth	1.84 m	5.52
12	103001001993AC00	11/06/2012	Worldview 2	Google Earth	1.84 m	5.52
13	1050410002DCCD00	21/09/2012	GeoEye-1	Google Earth	1.84 m	5.52
14	10600100080F0A00	25/03/2013	IKONOS 02	Google Earth	4 m	12
15	1050410002ACF600	14/06/2013	GeoEye-1	Google Earth	1.84 m	5.52
16	10504100023C1F00	24/08/2013	GeoEye-1	Google Earth	1.84 m	5.52
17	10600100087E0600	02/01/2014	IKONOS 02	Google Earth	4 m	12
18	1050410010327A00	19/03/2014	GeoEye-1	Google Earth	1.84 m	5.52
19	1050410010CD5400	06/07/2014	GeoEye-1	Google Earth	1.84 m	5.52
20	1050410012055800	05/01/2015	GeoEye-1	Google Earth	1.84 m	5.52
21	103001003F9C5C00	15/03/2015	Worldview 2	Google Earth	1.84 m	5.52
22	1040010010676900	05/08/2015	Worldview 3	Google Earth	1.24 m	3.72
23	1050010003041000	10/02/2016	GeoEye-1	Google Earth	1.84 m	3.72
24	104001001C9E8600	09/05/2016	Worldview 3	Google Earth	1.24 m	3.72
25	103001005C341600	18/09/2016	Worldview 2	Google Earth	1.84 m	5.52
26	105001000915F400	04/04/2017	GeoEye-1	Google Earth	1.84 m	5.52
27	1050010009409E00 1050010009409F00	15/04/2017	GeoEye-1	Google Earth	1.84 m	5.52
28	105001000A485B00 105001000A485C00	14/06/2017	GeoEye-1	Google Earth	1.84 m	5.52
29	1040010033D06D00	13/10/2017	Worldview 3	Google Earth	1.24 m	3.72
30	104001003819B400	15/02/2018	Worldview 3	Google Earth	1.24 m	3.72
31	10400100428C2B00	05/09/2018	Worldview 3	Google Earth	1.24 m	3.72
32	104001004A209500	01/05/2019	Worldview 3	Google Earth	1.24 m	3.72
33	104001004E761200	26/06/2019	Worldview 3	Google Earth	1.24 m	3.72
34	104001004F358D00	15/07/2019	Worldview 3	Google Earth	1.24 m	3.72

3.2. Methods for determining shorelines

Many approaches to monitor coastal change are often applied in the previous studies, including coastal charts and maps, historical photographs, beach surveys, aerial imagery, in situ geographic positioning system, satellite image processing, or elevation based, techniques (Boak and Turner 2005; Mullick et al., 2020). The extraction of shoreline from traditional ground survey techniques (surveys, geodetic measurements, etc.) usually takes time, effort, and money; sometimes challenging for a large region, although it can provide an accurate result (Mullick et al., 2020). The use of LiDAR (Light Detection and Ranging) technology

and video systems provide high accuracy but requires a large amount of funding (Turner et al., 2016). With the advent of space technology, remote sensing data has become a potential tool for geographical researches that provide a reasonably accurate estimate of shoreline. However, this technique becomes difficult in some tropical countries due to the frequent presence of clouds on optical sensors (Mullick et al., 2020). The radar satellite images from RADARSAT-1, Sentinel 1A have reasonable accuracy for distinguishing the land and water features (Al Fugura et al., 2011). But the limitation of these images is that their time range is not long enough (only since 2015) to detect the regularity (if any) of shoreline changes. Considering the need and interest in investigating the long-term temporal trend, LANDSAT satellite images offer high potential as the mission was launched in 1972 (Mullick et al., 2020). Therefore, LANDSAT satellite images have been wider potential to obtain shoreline patterns of any coast for a long-term temporal horizon. The advantages of using LANDSAT images over other methods are its availability without cost, ability to capture the large aerial extent, having a large temporal scale for historical shoreline change detection, etc. However, its disadvantage is that the spatial resolution is only average scale (30 m).

Geographic Information System (GIS) and Remote Sensing (RS) are often integrated for extracting and analyzing a coastal feature. The appearance of the water and land portion as a contrasting feature from satellite images is the prerequisite of shoreline delineation in the geospatial analysis (Mullick et al., 2020). Many change detection techniques based on the band ratio, band difference, post-classification of the image pixel is adopted for shoreline change analysis (El-Asmar and Hereher, 2011). For instance, the Normalized Difference Water Index (NDWI) can be used to distinguish land from the water (Gao, 1996; McFeeters, 1996). The NDWI is computed using the Green and the Near Infrared (NIR) wavelengths, defined by McFeeters (1996):

$$NDWI = (Green-NIR)/(Green+NIR) \quad (1)$$

The advantage of the NDWI index is that the needed bands of are available at all LANDSAT sensors. However, construction land and water surface sometimes can be mixed in the NDWI result. Based on the NDWI, Xu (2006) proposed Modified Normalized Difference Water Index (MNDWI). The MNDWI can be noted as follows (Xu, 2006):

$$MNDWI = (Green-MIR)/(Green+MIR) \quad (2)$$

where MIR is a middle infrared band.

The MNDWI has been verified by numerous studies that it is more likely to enhance information on the water so that the water surface can be extracted more accurately (Li et al., 2013; Xu and Guo, 2014). This is the method used to identify shoreline generations on LANDSAT images in 1990 and 2001. However, MIR band is not available in the LANDSAT MSS images especially in 1973. Therefore, the shoreline in 1973 is calculated using the NDWI.

To overcome the shortcomings of remote-sensing analysis with medium-resolution digital image processing, the study has combined the use of high-resolution satellite imagery of Google Earth (Table 1) to calculate shoreline changes. The satellite images obtained from Google Earth Pro software with a high spatial resolution and free, but they cannot be processed automatically like other satellite images. Therefore, the shorelines from 2002 to 2019 were manually digitized on Google Earth Pro software. Note that, in some areas, at some point in time, some Google Earth satellite images may be out of position compared to other periods in the same area. In the study area, the Google Earth provides satellite images (QuickBird-02), taken on April 21, 2002, and November 10, 2004, which are

dislocated from other periods. Therefore, after digitizing manually, the shorelines on 21/4/2002 and 10/11/2004 were adjusted by the Spatial Adjustment tool of ArcGIS 10.5 software before calculating the shoreline change rate.

3.3. Methods for calculating shoreline change

After applying the appropriate indicators to identify shorelines on different generations of maps and satellite images, the shoreline change rate is calculated using the Digital Shoreline Analysis System (DSAS) tool. DSAS is a freely available software application that works within the Esri Geographic Information System (ArcGIS) software. The DSAS computes rate-of-change statistics for a time series of shoreline vector data. The latest version is the DSAS 5.0, which was released in December 2018 (Himmelstoss et al., 2018). In this study, DSAS is performed in four steps: (1) preparation of shorelines, (2) creation of baselines, (3) creation of transects, and (4) calculation of shoreline change rate. Accordingly, this study used three calculation methods: End Point Rate (EPR), Linear Regression Rate (LRR), and Weighted Linear Regression (WLR). In addition, this study also calculates and analyzes supplemental statistics such as shoreline change envelope (SCE), standard error and R-squared statistic (R2), or the coefficient of determination, to evaluate the accuracy of the calculated results. The flowchart for calculating shoreline changes is shown in Fig. 2.

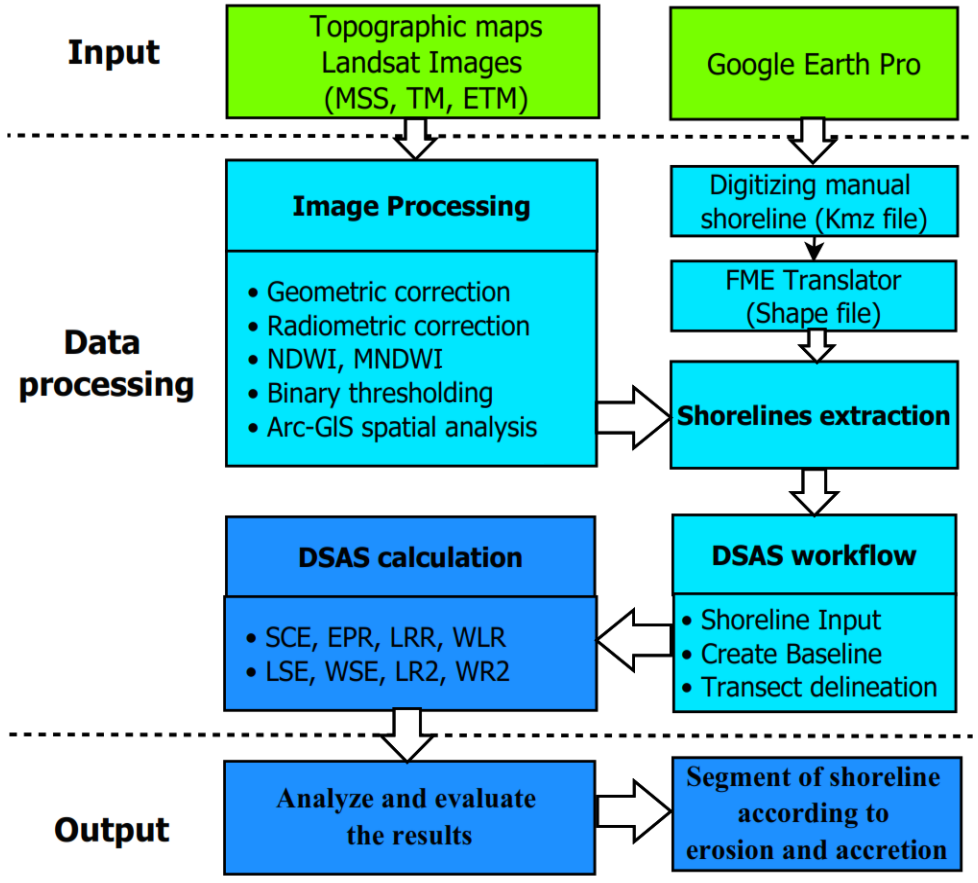

Figue 2. Flowchart of shoreline change assessment

End Point Rate

The end point rate (EPR) is calculated by dividing the distance of shoreline movement by the time elapsed between the oldest and the most recent shoreline (Fig. 3). The major advantages of the EPR are the ease of computation and minimal requirement of only two shoreline dates. The disadvantage is that in cases where more data are available, the additional information is ignored (Himmelstoss et al., 2018).

Linear Regression Rate

Regression is a mathematical model that expresses the change of a variable (dependent variable) according to one or more other variables (independent variable = explanatory variable). The simple linear regression model is calculated based on the formula:

$$Y = \beta iXi + \beta o \quad (3)$$

Where: Y is a dependent variable of the continuous form; Xi is an independent variable; βo is the intersection point of the regression line and Y axis; βi is the slope of the independent variable.

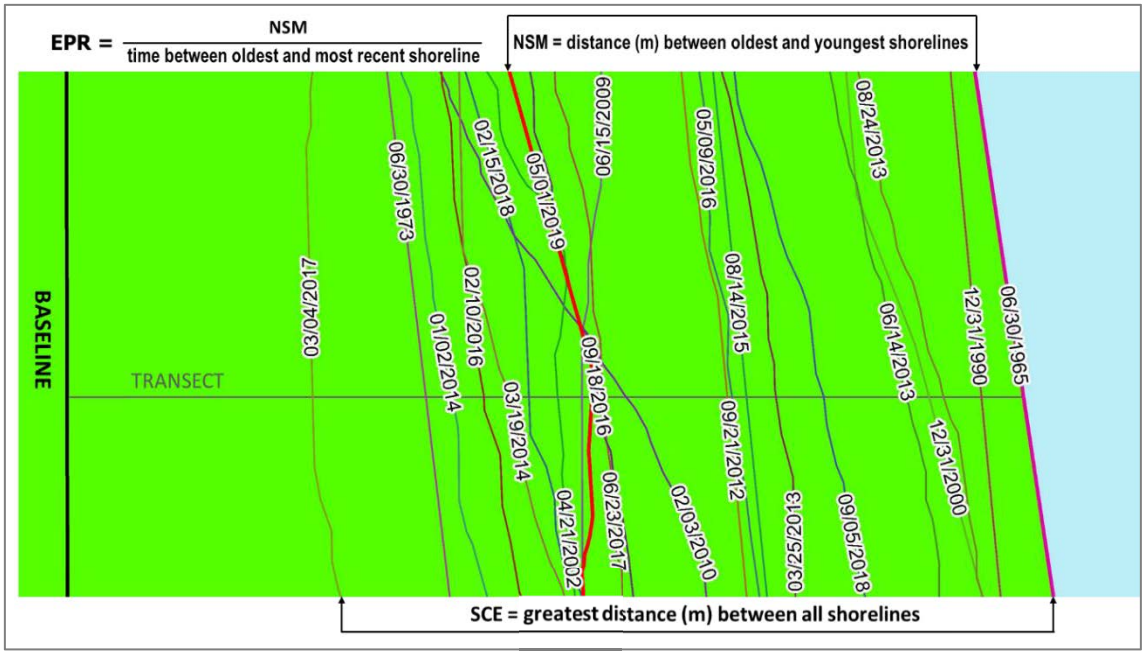

Figure 3. Simulation of SCE and EPR methods

In calculating shoreline changes, LRR is calculated through the slope of the linear regression line. The regression line is placed, so the sum of the squared residuals (determined by squaring the offset distance of each data point from the regression line and adding the squared residuals together) will be minimized (Himmelstoss et al., 2018) (Fig. 4). The linear regression rate is the slope of the line. The advantage of this method is that it is easy to calculate, all the data are used, regardless of changes in trend or accuracy, the method is purely computational, the calculation is based on accepted statistical concepts. Therefore, it is objective and gives more reliable results than the EPR method (Crowel et al., 1997; Mullick et al., 2020).

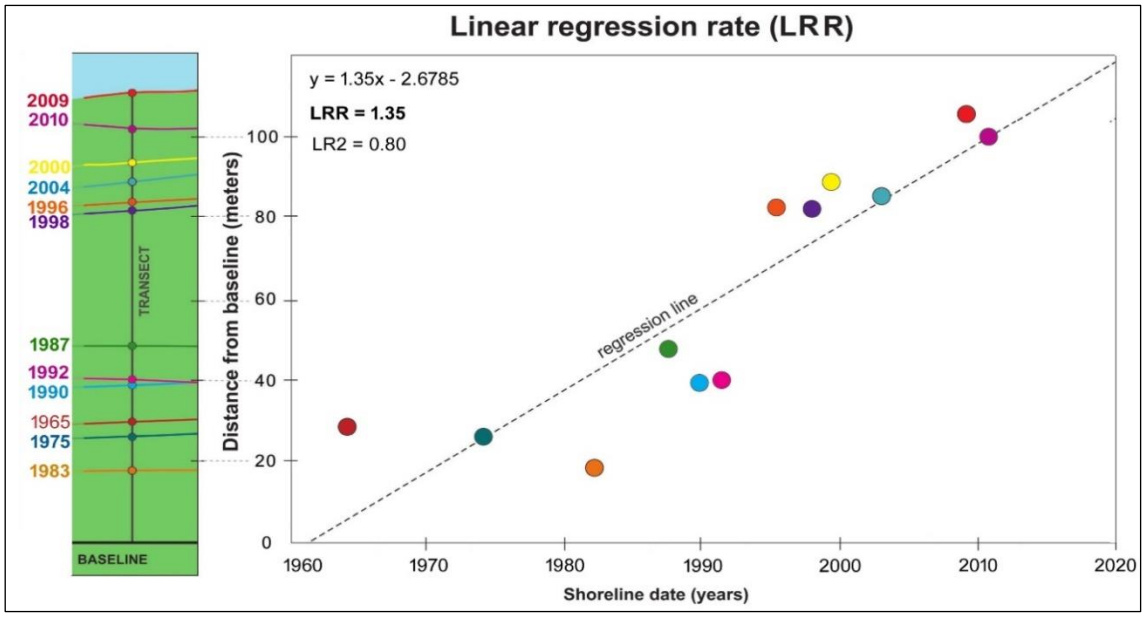

Figure 4. Simulating the LRR method. The slope of the equation (y = 1.35x-2.6785) describing the line is the rate (1.35 meters per year) of the shoreline at that section (Modified after Himmelstoss et al., 2018)

Weighted Linear Regression

WLR is a method of determining the regression equation based on the reliability of data. This method requires the user to declare the confidence level (uncertainty) in the attribute data of the shoreline. The uncertainty field of the shoreline feature class is used to calculate a weight. The weight (w) is defined as a function of the variance in the uncertainty of the measurement (e) (Genz et al., 2007):

$$w = 1/e^2 \quad (4)$$

where: "e" is shoreline uncertainty value.

Based on the weighted value (w), in a weighted linear regression, more reliable data are given greater emphasis or weight towards determining a best-fit line (Fig. 5). In the computation of rate-of-change statistics for shorelines, greater emphasis is placed on data points for which the position uncertainty is smaller. The WLR statistical method is more reliable because it takes into account the uncertainty field to calculate the long-term rates of shoreline change (Kankara et al., 2014).

Parameters to assess the reliability of the calculation results

In the DSAS tool, in addition to calculating the EPR, LRR and WLR, it also calculates parameters to assess the reliability of those results: uncertainty of end point rate method (EPRunc), standard error (LSE for ordinary linear regression and WSE for weighted linear regression) and correlation coefficient or R-squared statistic (R^2) (LR2 for the LRR and WR2 for the WLR). These additional statistics (EPRunc, LSE/WSE and LR2/WR2) are calculated using formulas 5, 6 and 7, respectively (Himmelstoss et al., 2018). These parameters provide information that is helpful in assessing the robustness of the computed regression rates.

$$EPRunc = \frac{\sqrt{(uncy\_A)^2 + (uncy\_B)^2}}{date\_A - date\_B} \quad (5)$$

Where: *uncy_A* is uncertainty from attribute field of shoreline A, *uncy_B* is uncertainty from attribute field of shoreline B, *date_A* is date of shoreline A (most recent), and *date_B* is date of shoreline B (oldest).

$$LSE\ or\ WSE = \sqrt{\frac{\Sigma(y-y')}{n-2}} \quad (6)$$

Where: y is known distance from baseline for a shoreline data point, y' is predicted value based on the equation of the best-fit regression line, and n is number of shorelines used.

$$R^2 = 1 - \sqrt{\frac{\Sigma(y-y)^2}{\Sigma(y-\bar{y})}} \quad (7)$$

Where: R^2 is the coefficient of determination, y is measured distance from baseline for a shoreline data point, y' is predicted distance from baseline based on the equation of the best-fit regression line, and $\bar{y}$ is mean of the measured shoreline distances from the baseline.

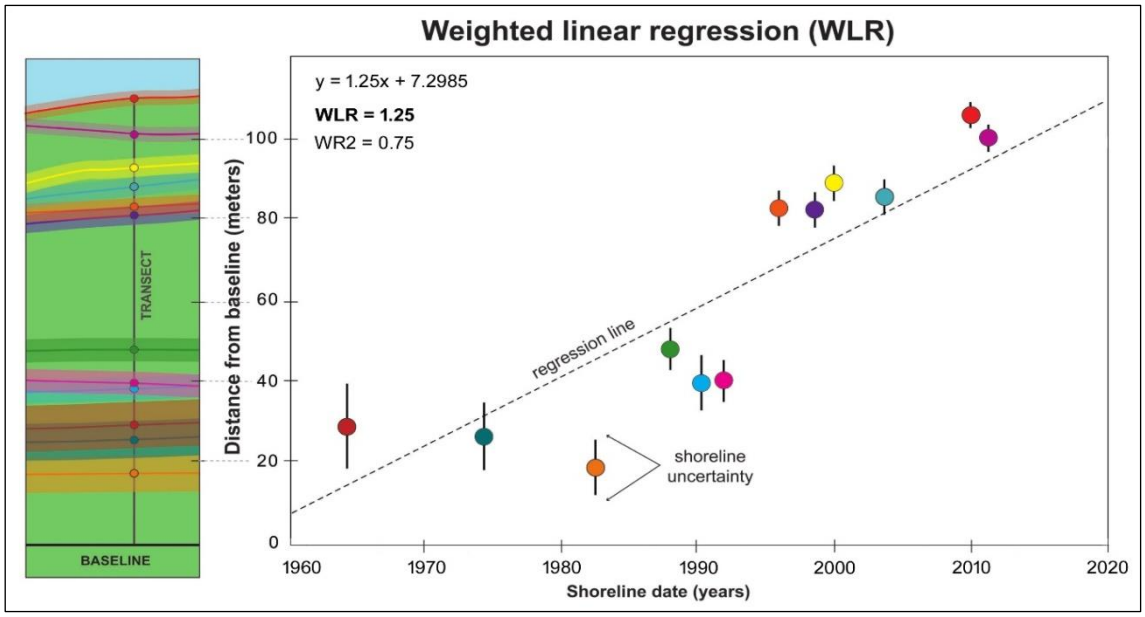

Figure 5. Simulating the WLR method. Smaller positional-uncertainty values (shown as vertical bars around each data point in the graph) have more influence in the regression calculation because of the weighting component in the algorithm. The slope of the equation (y = 1.25x-7.2985) describing the line is the rate (1.25 meters per year) of the shoreline at that section (Modified after Himmelstoss et al., 2018)

4. Results

In Son Tra - Cua Dai area, 1647 transects were constructed perpendicular to the shorelines and baselines with a distance between them of 20 m (Fig. 6). According to the calculation results, in about 54 years (from 1965 to 2019) the shoreline changes envelope (SCE) in this area reaches a maximum of 512 m and a minimum of 20 m (Table 5). In order to better understand the process of shoreline changes associated with natural and human activities in the area at different times, in addition to an overall assessment of the rate of shoreline changes from 1965 to 2019, the study was divided into three smaller stages, from 1965 to 2002, from 2002 to 2012 and from 2012 to 2019. This study followed all three calculation methods: EPR, LRR, and WLR. The main parameters of calculation results and related indicators are shown in Tables 2-5. The comparison of accuracy between the results calculated according to the method is shown in Fig. 7. Accordingly, the WLR method in all periods produced results that were much more reliable than the LRR method (Fig. 7). Therefore, this study will use WLR results to analyze and assess the shoreline changes in the study area. The results of the shoreline change rate for each period are presented below.

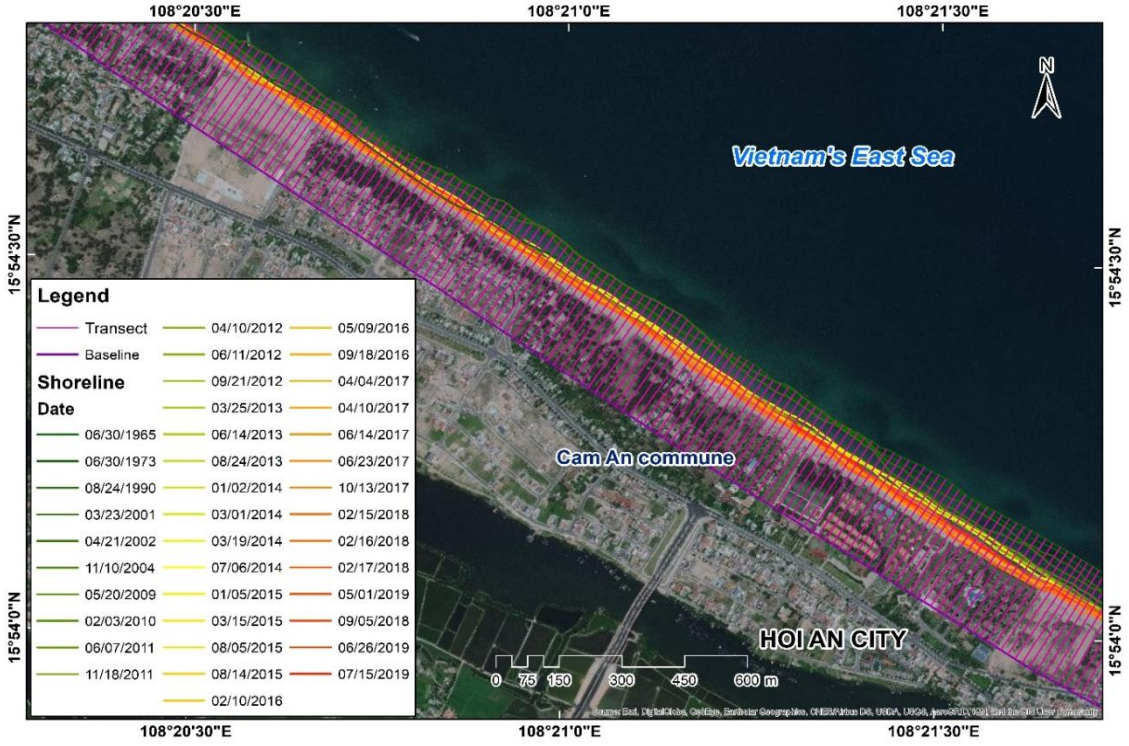

Figure 6. A representative part of the Son Tra - Cua Dai area showing the baselines, shorelines and transects (distance between transects is 20 m)

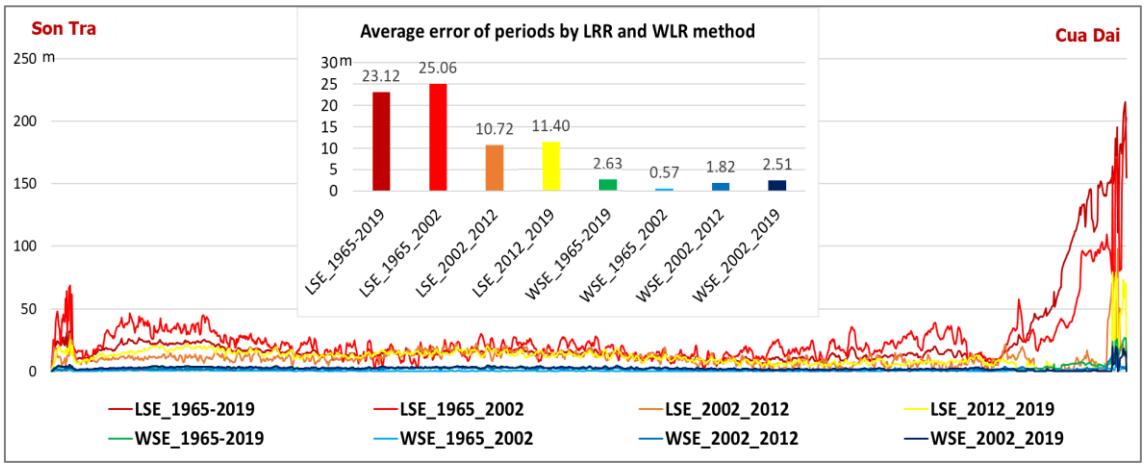

Figure 7. Distribution of errors by the WLR (WSE) and LRR (LSE) methods in the calculation results from 1965 to 2019

4.1. The shoreline change rate from 1965 to 2002

Calculation results show that the SCE in the period from 1965 to 2002 was 450 m and the average value reached 70 m. The results of the three methods EPR, LRR, and WLR are basically quite similar. According to the WLR method, the maximum erosion rate in the area

reaches 2.2 m/year and the strongest accretion reached 9.5 m/year. Statistical results show that the number of transects with erosion tendency (erosion rate > 0.2 m/year) is 676/1647, accounting for 41%; the number of transects with accretion tendency (the rate of accretion > 0.5 m/year) is 363/1647, accounting for 22%; the remaining 37% were transected showing relative stability of the coast (Table 2). In which, the area with strong erosion rate is Cam An commune, Hoi An city.

Table 2. Statistical table of some basic parameters according to different methods, period 1965-2002

Objects	Temporal segment 1965-2002								
	SCE	**EPR**	*EPRu*	**LRR**	LR^2	*LSE*	**WLR**	WR^2	*WSE*
Min	5.96	**-1.76**	*1.54*	**-1.54**	*0.00*	*1.71*	**-2.21**	*0.00*	*0.03*
Max	450.74	**9.10**	*2.37*	**10.24**	*0.96*	*202.8*	**9.54**	*0.96*	*4.15*
Mean	69.91	**0.45**	*1.59*	**0.83**	*0.31*	*25.06*	**0.20**	*0.23*	*0.57*
Transect_E (V < -0.2 m/year) (%)	-	**27.08**	-	**12.02**	-	-	**41.04**	-	-
Transect_A (V > 0.5 m/year) (%)	-	**32.06**	-	**51.25**	-	-	**22.04**	-	-
Transect_S (-0.2 < V < 0.5 m/year) (%)	-	**40.86**	-	**36.73**	-	-	**36.92**	-	-

where: SCE, EPRu-uncertainty of EPR, LSE and WSE-standard error of LRR and WLR (m); EPR, LRR and WLR (m/year); Transect_E-erosion transects, Transect_A-accretion transects and Transect_S-stability transects (%)

4.2. The shoreline change rate from 2002 to 2012

According to the statistics in Table 3, the SCE of the shoreline from 2002 to 2012 was ~179 m, and the average value was ~38 m. The results of the WLR method show that the maximum erosion rate in the area reaches 24.8 m/year (10 times higher than the period from 1965 to 2002) and the strongest accretion reaches 19.4 m/year. In this period, accretion activities predominate with 65.4% of transects; erosion activities were only observed in 20% of transects, but the intensity of erosion is particularly strong compared to the previous period.

Table 3. Statistical table of some basic parameters according to different methods, period 2002-2012

Objects	Temporal segment 2002-2012								
	SCE	**EPR**	*EPRu*	**LRR**	LR^2	*LSE*	**WLR**	WR^2	*WSE*
Min	179.3	**-24.18**	*0.00*	**-24.84**	*0.00*	*0.00*	**-24.77**	*0.00*	*0.00*
Max	0.55	**19.17**	*3.54*	**19.45**	*1.00*	*98.09*	**19.35**	*1.00*	*17.73*
Mean	37.66	**-2.87**	*1.26*	**-2.21**	*0.53*	*8.10*	**-2.28**	*0.49*	*1.44*
Transect_E (V <-0.2m/year)	-	**22.77**	-	**19.06**	-	-	**19.91**	-	-
Transect_A (V > 0.5m/year)	-	**69.28**	-	**65.45**	-	-	**65.39**	-	-
Transect_S (-0.2 <V < 0.5m/year)	-	**7.59**	-	**15.49**	-	-	**14.70**	-	-

where: SCE, EPRu - uncertainty of EPR, LSE and WSE - standard error of LRR and WLR are in (m); EPR, LRR and WLR are in (m/year); Transect_E - erosion transects, Transect_A - accretion transects and Transect_S - stability transects are in (%)

4.3. The shoreline change rate from 2012 to 2019

Table 4 shows that the SCE reached 362 m, the average value reached 38.5 m. According to the WLR method, the maximum erosion rate in the area reaches to 78 m/year (more than three times in the period of 2002-2012 and more than 35 times in the period of 1965-2002), and the strongest accretion reaches 29.7 m/year. In this period, the percentage of erosion sections (33.6%) was still smaller than the accretion transects (45.5%), but the intensity of erosion was particularly strong, the strongest compared to previous periods.

Table 4. Statistical table of some basic parameters according to different methods, period 2012-2019

Objects	Temporal segment 2012-2019								
	SCE	**EPR**	*EPRu*	**LRR**	LR^2	*LSE*	**WLR**	WR^2	*WSE*
Min	0.5	**-75.42**	*1.11*	**-74.26**	*0.00*	*0.00*	**-78.13**	*0.00*	*0.00*
Max	362.3	**28.12**	*1.21*	**29.76**	*0.98*	*79.39*	**29.76**	*0.98*	*19.63*
Mean	38.54	**0.70**	*1.17*	**-0.63**	*0.15*	*11.4*	**-0.45**	*0.15*	*2.51*
Transect_E (V <-0.2m/year)	-	**20.58**	-	**34.06**	-	-	**33.64**	-	-
Transect_A (V > 0.5m/year)	-	**56.83**	-	**40.01**	-	-	**45.48**	-	-
Transect_S (-0.2 <V < 0.5m/year)	-	**22.59**	-	**25.93**	-	-	**20.89**	-	-

where: SCE, EPRu - uncertainty of EPR, LSE and WSE - standard error of LRR and WLR are in (m); EPR, LRR and WLR are in (m/year); Transect_E-erosion transects, Transect_A-accretion transects and Transect_S-stability transects are in (%)

4.4. The shoreline change rate from 1965 to 2019

The results of the shoreline changes in the 1965-2019 period are summarized as shown in Table 5 and Fig. 8. Accordingly, in this period, the strongest erosion activity mainly concentrated in the northern area of Cua Dai, Hoi An city. In which, the highest erosion speed is about 40 m/year. The other areas are mainly active in accretion (53.5% transects) (Fig. 8). According to the statistics shown in Table 5, within 54 years, the greatest distance between all shorelines is 512 m (SCE) and the average value in this area is about 84 m.

Table 5. Statistical table of some basic parameters according to different methods, period 1965 - 2019

Objects	Temporal segment 1965-2019								
	SCE	**EPR**	*EPRu*	**LRR**	LR^2	*LSE*	**WLR**	WR^2	*WSE*
Max	512	**5.05**	*1.21*	**7.51**	*0.92*	*215.4*	**4.32**	*0.74*	*27.06*
Min	20.5	**-2.09**	*1.11*	**-2.85**	*0.00*	*6.23*	**-42.74**	*0.00*	*0.52*
Mean	83.9	**0.3**	*1.12*	**-0.07**	*0.16*	*23.12*	**-0.41**	*0.15*	*2.63*
Transect_E (V <-0.2m/year)	**-**	**14.75**	-	**42.14**	-	-	**25.99**	-	-
Transect_A (V > 0.5m/year)	**-**	**39.10**	-	**15.79**	-	-	**53.55**	-	-
Transect_S (-0.2 <V < 0.5m/year)	**-**	**46.15**	-	**42.07**	-	-	**20.46**	-	-

where: SCE, EPRu - uncertainty of EPR, LSE and WSE - standard error of LRR and WLR are in (m); EPR, LRR and WLR are in (m/year); Transect_E - erosion transects, Transect_A - accretion transects and Transect_S - stability transects are in (%)

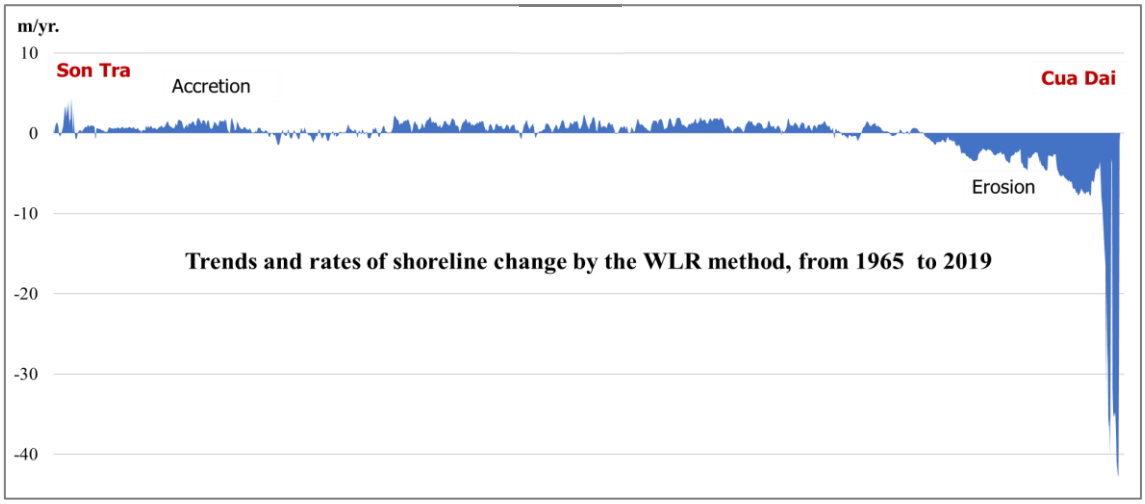

Figure 8. Trends and rates of shoreline change by the WLR method, period from 1965 to 2019 in Son Tra - Cua Dai area

4.5. Segmentation of the Son Tra - Cua Dai coast according to the erosion rate for setback zone establishment

Based on the calculation results of shoreline changes from 1965 to 2019, the study has conducted the coastal segment according to the erosion/accretion characteristics of the Son Tra - Cua Dai area. In the classification of erosion/accretion, Himmelstoss et al., (2018), divided the calculated values into nine different levels, of which four levels belong to erosion group (negative group), four levels belong to accretion group (positive group) and one level for relative stability (Table 6).

Table 6. Determining the breaks for data values according to Himmelstoss et al., (2018)

No	Rate of change (m/year) (EPR, LRR, WLR)	Group
1	Min < ─ <= -3.0	Negative
2	-3.0 < ─ <= -2.0	
3	-2.0 < ─ <= -1.0	
4	-1.0 < ─ <= -0.5	
5	-0.5 < ─ <= 0.5	Stability
6	0.5 < ─ <= 1.0	Positive
7	1.0 < ─ <= 2.0	
8	2.0 < ─ <= 3.0	
9	3.0 < ─ <= Max	

Based on the erosion/accretion classification of Himmelstoss et al., (2018) and the characteristics of Son Tra - Cua Dai area (there are sections of the coast with very high erosion rate along with that there is a huge difference in value between the highest erosion rate and the highest accretion rate, the difference is ~ 10 times, Table 5) and the goal of this study is to serve the coastal setback establishment. Therefore, the study should pay special attention to erosion values. This study has divided the values of the shoreline change rate as shown in Table 7. Accordingly, the coast of Son Tra - Cua Dai area is divided into 30 segments and grouped into 8 groups with different erosion/accretion characteristics: accretion, relative stability, erosion and accretion alternately, weak erosion, moderate erosion, strong erosion, very strong erosion and super strong erosion (which can become "disaster") (Table 7, Fig. 9). In particular, the accretion segments were dominated with ~ 16.5 km, accounting for 49.4%; followed by the segments with erosion and accretion activities alternating and a total length of ~ 5 km, accounting for 15%; next is the weak erosion segments with a length of ~ 4.2 km, accounting for 12.6%; the segments of erosion averages ~ 2.3 km, accounting for ~ 6.9%; the relative stability segments had a total length of ~ 2.1 km, accounting for about 6.3%. The segments with strong, very strong to super-strong erosion have a total length of ~ 3.3 km and account for ~ 9.9% and they are concentrated mainly in the southern part of the study area (Cua Dai area) (Fig. 9).

Table 7. Statistical table of shoreline characteristics in Son Tra - Cua Dai area according to the shoreline changes rate

No	Code	Rate of erosion/accretion (m/year)	Erosion/accretion level	Length (total) (km)	Ratio %
1	0	> 0.5	Accretion	16.5	49.4
2	1	(-0.2)-0.5	Relative stability	2.1	6.3
3	2	-	Erosion and accretion alternately	5.0	15.0
4	3	(-0.2)-(-1.5)	Weak erosion	4.2	12.6
5	4	(-1.5)-(-3.0)	Moderate erosion	2.3	6.9
6	5	(-3.0)-(-5.0)	Strong erosion	1.6	4.8
7	6	(-5.0)-(-10.0)	Very strong erosion	1.2	3.6
8	7	< -10.0	Super strong erosion	0.5	1.5
	Total			33.4	100.0

5. Discussions

5.1. Factors affecting the shoreline identification

In this study, the shoreline obtained from remote sensing images is an immediate shoreline, defined as an intersected line between land and sea at a particular time (Wicaksono et al., 2018). It is the boundary between the beach and the water level (tidal) when the satellite images were taken. Therefore, it will be influenced by tidal levels. In order to minimize the impacts of tidal, it is usually necessary to take some steps such as select satellite images at the same time in different years and the highest spatial resolution possible, calculate the tide level difference to adjust the shoreline accordingly, using multiple shorelines at different times, and linear regression methods to calculate the shoreline change, etc.

When considering the shoreline changes according to satellite image data, the biggest obstacle is the difference in image recording times (Kelly and Gontz, 2018). Because at different times, the satellite image will show a different shoreline position, depending on the tidal fluctuation. Depending on the tidal changes in a day and the coastal geometry, the shoreline can change from centimeters to hundreds of meters horizontally (Wicaksono et al., 2018). However, when examining and analyzing the influence of the tides on the determination of the shoreline on the satellite image in the area where the tidal fluctuation level is not large (~1 m), and the beach has a great slope, Wicaksono et al. (2018) indicated the shoreline position change after tidal correction only varied from 0.21 m to 1.8 m. Therefore, according to Wicaksono et al. (2018), tidal correction in areas with the above characteristics is not necessary, especially when using satellite images with spatial resolution more than 3 m.

The natural condition in the case of the Son Tra - Cua Dai coastal region has many similarities with the study area of Wicaksono et al. (2018). This area is located in the area with the smallest tidal range in Vietnam (from 0.8 m to 1.2 m) (Lam, 2009; Tung, 2011) and the beach is the high slope, so the tidal influence is not too great. In fact, as calculated by Cham et al., (2020) for the Cua Dai area (the southern part of the study area), it shows that the difference in shoreline between before and after the tidal adjustment varies from 0.62 to 16.27 m. These values are not large if compared with the spatial resolution of the satellite images used by Cham et al., (2020) in the calculation, from 10 m to 60 m. Therefore, the use of very-high-resolution remote sensing images as used in this study have become a potential solution for monitoring shoreline changes. Especially, the multi-temporal remote sensing images available in the Google Earth system provided 30 shorelines from 2002 to 2019. All images have very high resolution (from 1.24 m to 4 m) including QuickBird 2, GeoEye-1, Iknos 02, Worldview 2, 3. This is an important parameter to evaluate the accuracy of the interpreted shorelines. In the WLR method, the accuracy of the shoreline will be declared to determine the weights in the construction of the regression equation (according to Equation 4, Genz et al., 2007). When calculating by WLR method, there are studies using image resolutions as the uncertainty to calculate weighting values (Mullick et al., 2020). In this study, in order to increase the confidence level for the calculation of WLR, authors declared the uncertainty value equal to three times the spatial resolution of satellite images (except that the shoreline in 1973 and the shorelines in 1965, 1990 and 2001 were one and two times, respectively) (Table 1). The results are in harmony with the erosion and accretion trends in the study area in recent decades, especially the significant erosion in the south part of research areas (near Cua Dai area), a slight erosion in the middle part and stable shoreline in the northern part (Fig. 9).

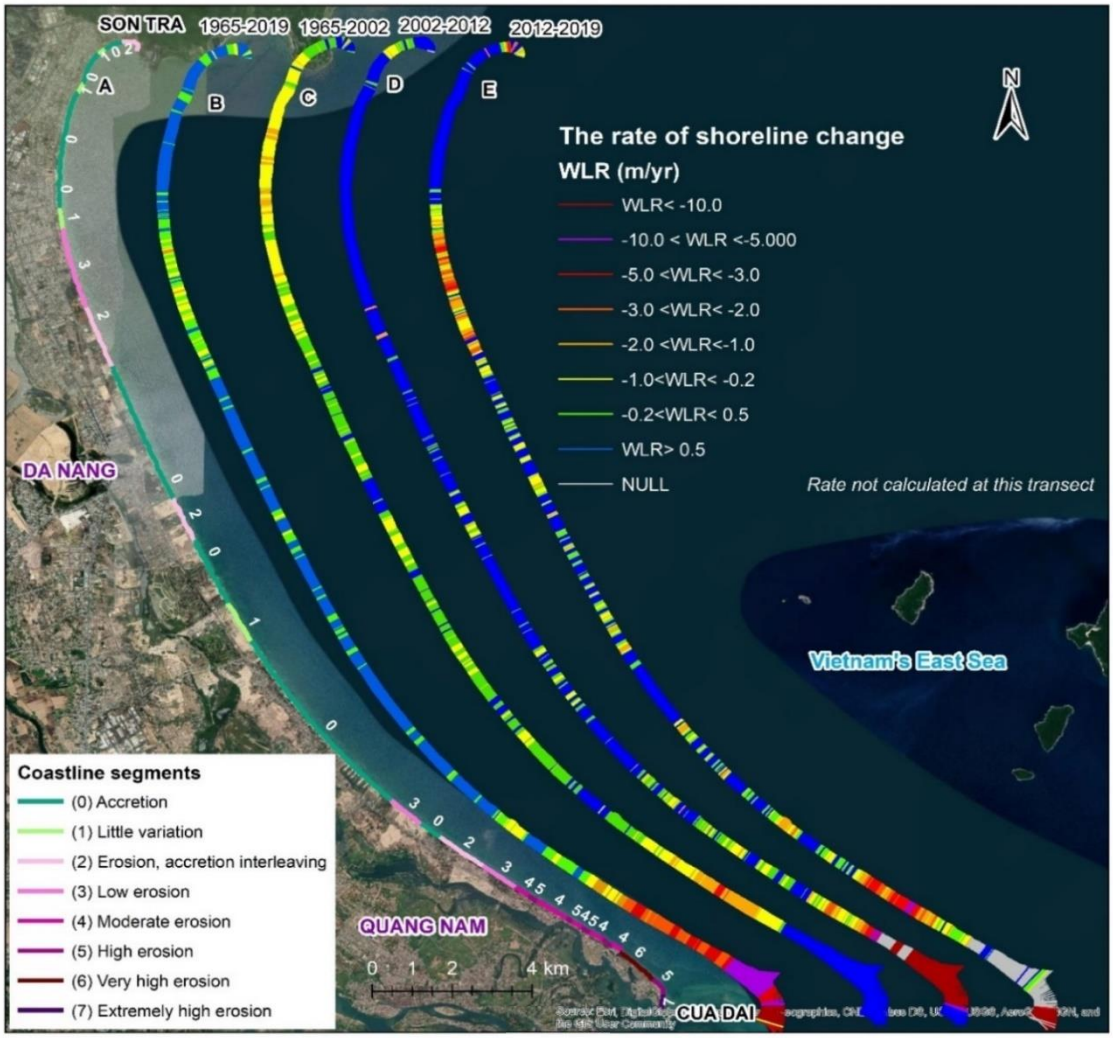

Figure 9. The results of shoreline changes in Son Tra - Cua Dai area: (A) coastal segments according to erosion/accretion characteristics and shoreline change rate, including periods: (B) from 1965 to 2019, (C) from 1965 to 2002, (D) from 2002-2012 and (E) from 2012-2019

5.2. Shoreline changes from 1965 to 2019

The shoreline-change results based on the EPR, LRR, and WLR methods shown in Tables 2, 3, 4, and 5 are similar to the Max, Min, and Mean values in three periods: from 1965 to 2002; from 2002 to 2012; and from 2012 to 2019. The assessment of shoreline changes in a short period can consist of some uncertainties due to specific natural conditions at the time when the satellite images were taken. However, these assessments play an important role to compare the shorelines in different land-use policy periods. Particularly, the period from 1965 to 2002 was chosen because human economic development activities in the region did not have significant impacts on the shore/beach. The fluctuations of the coast mainly were come from natural effects. From 2002 to 2012, the coastal areas were impacted by local economic

development activities and extreme weather events, especially with typhoons. In particular, the typhoon No. 9 happen in 2009 (known as Ketsana typhoon) was considered as the strongest storm within 40 years (since 1969) in the study area (Van et al., 2013; Thai et al., 2018). In addition, the construction of coastal tourism centers has partly affected regional beaches and imbalanced the natural ecosystems in the research area. It has led to the increase of coastal erosion in the Cua Dai part, Hoi An City, with 104 sides with erosion speed of 10-24 m/year; 58 sections with erosion speed of 3-10 m/year (Figs. 9d, 10b). In the period of 2012-2019, the impacts of human economic development activities on the shore/beach were significantly increased. The quick expansion of beach/beach resort centers has impacted on the natural ecosystems. The strongest erosion was identified in the Cua Dai part with an erosion speed of 70-80 m/year (Fig. 9e, 10c, Table 4).

Figure 10. Trends and rates of shoreline change in Son Tra - Cua Dai area by the WLR method, in the periods: (a) from 1965 to 2002; (b) from 2002 to 2012 and (c) from 2012 to 2019

In the period from 1965 to 2019, the shoreline change assessments based on three methods were shown in Table 5. The assessments based on the EPR method only show the two shorelines in 1965 and 2019, instead of showing the shoreline changes in recent years. The assessments based on the LRR method have different levels of confidence (Table 1), but they are not included in the calculation due to the

shorelines have the same weight. In Google Earth software, the images taken during the last 10 years have higher resolution than those taken before the year 2000s, leading the correction in shoreline identification. The assessments based on the WLR method using a linear regression formulation give priority to high-precision data sets first and gradually lower the priority for lower-precision data sets. In other words, the more the shorelines in recent years have become more and more accurate, the higher the weight of the regression calculation for the shorelines of this period. Therefore, the WLR method results show the highest accuracy (Fig. 7), compared to two others (Figs. 7, 9b, d, e, and Fig. 10b, c).

5.3. The role of coastal erosion research in setback zone establishment

One of the most important functions of a coastal setback zone is to minimize damage from coastal erosion (VNA, 2015). It has been used effectively in the Barcelona Convention on Coastal Area Management of the Convention, active since 24 March 2011 (UNEP, 2008). The establishment of setback zones requires an adjustment of development activities in high-erosion risk areas towards an effective integrated coastal management (Knecht, 1997). According to Linham and Nicholls (2010), the history of coastal erosion is an indispensable content to identify global setback zones. Based on the DSAS tool, the study has calculated the speed/evolution of the shoreline in the Son Tra - Cua Dai area in the history of about 55 years (from 1965 to 2019) (Table 5). Afterward, the position of the shoreline in the planning periods was done in this study. The DSAS tool allows the prediction of future shoreline locations according to the Kalman model (Kalman, 1960) and developed by Long and Plant (2012) (Himmelstoss et al., 2018). Accordingly, the study formulated a shoreline change scenario for the Son Tra - Cua Dai area over the next 20 years (to 2041) as shown in Fig. 11. Accordingly, the research area in Da Nang province seems to be stable, compared to the shoreline in 2019. The predicted shoreline in 2041 in Cam An district will be eroded from the Palm Garden resort to the Cua Dai region with a distance from 80 m to 200 m. The most erosion risk can be found in the southern part of the study area, near Hoi An City with erosion distance up to 200 m (Fig. 11). The establishment of setback zones in Vietnam can be a potential tool to minimize the physical and economic impacts of coastal natural disasters in the future (UNEP/GPA, 2009).

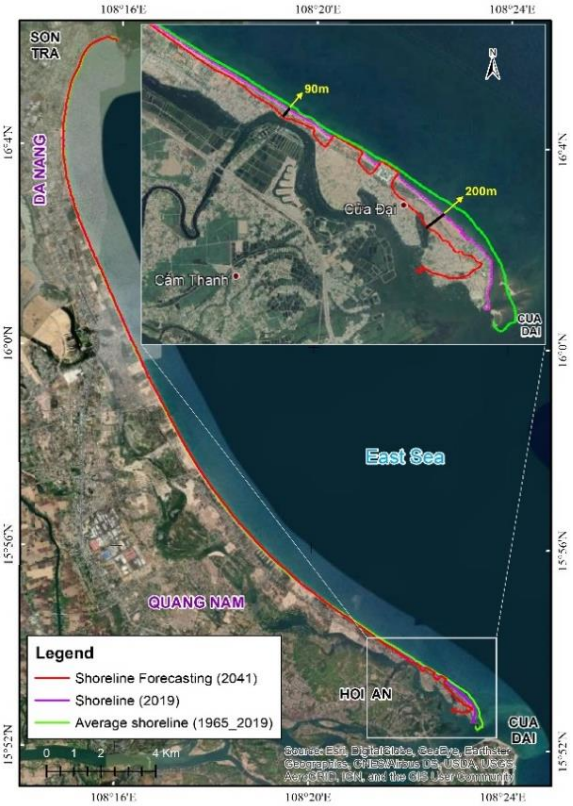

Figure 11. Shoreline forecasting after 20 years (to 2041) in Son Tra - Cua Dai area

6. Conclusions

Three methods of EPR, LRR, and WLR can be used effectively in this study to

calculate the shoreline fluctuations. For analysis in a short time and confident shorelines, the calculation results of the three methods EPR, LRR, and WLR are basically similar. For long periods, with many generations of shorelines, the WLR method provides higher accuracy and efficiency than two others. Therefore, the study recommends using the WLR method to calculate shoreline variation in other studies.

Based on three quantitative methods, the shoreline changes of the Son Tra - Cua Dai area is complicated. From 1965 to 2002, the shorelines were slightly eroded in the northern part of Hoi An, while strong deposition was identified in the southern part of Son Tra and the northern part of the Cua Dai area. From 2002 to 2012, the coastal areas in the southern part of Son Tra had accretion trend. The central area of Son Tra - Cua Dai is more stable than two other sides. In the period of 2012 to 2019, the coastal parts in the Cua Dai area and Hoi An City were eroded strongly.

Son Tra - Cua Dai coast can be divided into 30 sections, which are clustered into 8 groups according to the erosion/accretion characteristics. In particular, the accretion sections (1) are dominated with a length of about 16.5 km, accounting for 49.4%; followed by the erosion-accretion sections (2) with a length of about 5 km, accounting for 15%; the very weak-eroded section (3) with a length of about 4.2 km, accounting for 12.6%; the weak-eroded sections (4) with a length of about 2.3 km, accounting for 6.9%; the moderate-eroded sections (5) with a length of about 2.1 km, accounting for 6.3%; the strong-eroded sections (6), extreme strong-eroded (7) and disaster-level (8) sections with a total length of about 3.3 km and accounting for ~ 9.9% of the total length of the coast in the area.

An erosion from 90 m to 200 m was predicted for the shoreline in Hoi An city in the next 20 years (until 2041). Therefore, it is necessary to establish an effective setback zone with the inner boundary from 90 m to 200 m inland in this area to minimize damage from coastal erosion in the future.

Acknowledgments

This study was supported by a national scientific and technological project, No. KC.09.17/16-20 funded by the Ministry of Science and Technology in Vietnam. We are thankful to the VNU University of Science, Hanoi for providing all the facilities for this research. We are grateful for the time and efforts of the editors and the anonymous reviewers on improving our manuscript.

References

Aiello A., Canora F., Pasquariello G., Spilotro G., 2013. Shoreline variations and coastal dynamics: a space-time data analysis of the Jonian littoral, Italy. Estuar Coast Shelf Sci., 129, 124–135. https://doi.org/10.1016/J.EcSS.2013.06.012.

Al Fugura A., Billa L., Pradhan B., 2011. Semi-automated procedures for shoreline extraction using single RADARSAT-1 SAR image. Estuar Coast Shelf Sci., 95, 395–400. https://doi.org/10.1016/TECSS.2011. 10.009.

Anh V.T., 2010. Study on morphodynamic dynamics of Thu Bon estuary. Ph.D. Thesis. Vietnam National University, Hanoi (in Vietnamese with English abstract).

Aouiche I., Daoudi L., Anthony E.J., Sedrati M., Ziane E., Harti A., Dussouillez P., 2016. Anthropogenic eiĩects on shoreface and shore- line changes: input from a multi-method analysis, Agadir Bay, Morocco. Geomorphology, 254, 16–31. https://doi.org/10.1016/J. GEOMORPH.2015.11.013.

Boak E.H., Turner I.L., 2005. Shoreline definition and detection: A Review. Journal of Coastal Research, 21(4(214)), 688–703. Doi: https://doi.org/10.2112/03-0071.1.

Cham D.D., 2020. Effects of hydrodynamical regime on morphological evolution at Cua Dai estuary and coastlines of Quang Nam province. Vietnam Journal of Earth Sciences, 42(2), 176–186. https://doi.org/10.15625/0866-7187/42/2/15005.

Cham D.D., Son N.T., Minh N.Q., Thanh N.T., Dung T.T., 2020. An Analysis of Shoreline Changes Using

Combined Multitemporal Remote Sensing and Digital Evaluation Model. Civil Engineering Journal, 6(1), 1–10.

El-Asmar H.M., Hereher M.E., 2011. Change detection of the coastal zone east of the Nile Delta using remote sensing. Environ Earth Sci., 62, 769–777. https://doi.org/10.1007/s12665-010-0564-9.

Gao B., 1996. NDWI - A normalized difference water index for remote sensing of vegetation liquid water from space. Remote Sens Environ, 58, 257–266. https://doi.org/10.1016/S0034-4257(96)00067-3.

Genz A.S., Fletcher C.H., Dunn R.A., Frazer L.N., Rooney J.J., 2007. The predictive accuracy of shoreline change rate methods and alongshore beach variation on Maui, Hawaii: Journal of Coastal Research, 23(1), 87–105.

Gupta N., Bhaskaran P.K., Dash M.K., 2015. Recent trends in wind-wave climate for the Indian Ocean. Curr Sci., 108, 2191–2201.

Hai T.T., 2017. Tectonic activities in the central coastal region of Vietnam and impact on geological disasters. Science and Technology Publishing House. ISBN: 978604670969-5. Hanoi, Vietnam (in Vietnamese).

Hakkou M., Maanan M., Belrhaba T., El Khalidi K., El Ouai D., Benmohammadi A., 2018. Multi-decadal assessment of shoreline changes using geospatial tools and automatic computation in Kenitra coast, Morocco. Ocean Coast Manag., 163, 232–239. https://doi.org/10.1016/j.ocecoaman.2018.07.003.

Himmelstoss E.A., Henderson R.E., Kratzmann M.G., Farris A.S., 2018. Digital Shoreline Analysis System (DSAS) version 5.0 user guide: U.S. Geological Survey Open-File Report. 2018–1179, 110p. https://doi.org/10.3133/ofr20181179.

Kalman R., 1960. A New Approach to Linear Filtering and Prediction Problems. ASME Journal of Basic Engineering, 82, 35–45. http://dx.doi.org/10.1115/1.3662552.

Kankara R.S., Chenthamil Selvan S., Rajan B., Arockiaraj S., 2014. An adaptive approach to monitor the Shoreline changes in ICZM framework: A case study of Chennai coast. Indian Journal of Marine Sciences, 43(7), 1266–1271.

Kelly J.T., Gontz A.M., 2018. Using GPS-surveyed Intertidal Zones to Determine The Validity of Shorelines Automatically Mapped by Landsat Water Indices. International Journal of Applied Earth Observation and Geoinformation, 65, 92–104.

Knecht R.W., 1997. Integrated Coastal Zone Management for Developing Maritime Countries. In B.U. Haq, S.M. Haq, G. Kullenberg, J.H. Stel (Eds.), Coastal Zone Management Imperative for Maritime Developing Nations (29–42). Springer Netherlands. https://doi.org/10.1007/978-94-017-1066-4_2.

Kuleli T., Guneroglu A., Karsli F., Dihkan M., 2011. Automatic detection of shoreline change on coastal Ramsar wetlands of Turkey. Ocean Eng., 38, 1141–1149.

Lam N, 2009. Hydrodynamics and Morphodynamics of a Seasonally Forced Tidal Inlet System, s.l.: Ph.D. Thesis, Delft University of Technology.

Li W., Du Z., Ling F., Zhou D., Wang H., Gui Y., Sun B., Zhang X., 2013. A Comparison of Land Surface Water Mapping Using the Normalized Difference Water Index from TM, ETM+ and ALI. Remote Sensing, 5(11), 5530–5549.

Linham M.M., Nicholls R.J., 2010. Technologies for climate change adaptation: Coastal erosion and flooding (TNA Guidebook Series) New Delhi, IN. UNEP Risø Centre on Energy, Climate and Sustainable Development, 150p.

Long J.W., Plant N.G., 2012. Extended Kalman Filter framework for forecasting shoreline evolution: Geophysical Research Letters, 39(13), 1–6.

Mau L.D. (editor), et al., 2014. Characteristics of erosion and deposition of coastal zone in Quang Nam. Publishing House of Natural Sciences and Technology (in Vietnamese).

Mau L.D., 2012. Computation of net longshore sediment transport rate in the Cua Dai (Hoi An) area. Vietnam Journal of Marine Science and Technology, 1, 27–42 (in Vietnamese with English abstract).

McFeeters S.K., 1996.The use of the normalized difference water index (NDWI) in the delineation of open water features. Int J Remote Sens., 17, 1425–1432. https://doi.org/10.1080/01431169608948714.

MONRE (Ministry of Natural Resources and Environment, Vietnam), 2016. Technical regulation for coastal setback zone establishment. No. 29/2016/TT-BTNMT (in Vietnamese).

Moussaid J., Ait A., Zourarah B., Maanan M., 2015. Using automatic computation to analyze the rate of shoreline change on the Kenitra coast, Morocco.

Ocean Eng., 102, 71–77. https://doi.org/10.1016/j.oceaneng.2015.04.044.

Mullick M.R.A., Islam K.M.A., Tanim A.H., 2020. Shoreline change assessment using geospatial tools: a study on the Ganges deltaic coast of Bangladesh. Earth Sci. Infor., 13, 299–316. https://doi.org/10.1007/s12145-019-00423-x.

Natesan U., Parthasarathy A., Vishnunath R., Kumar G.E.J., Ferrer V.A., 2015. Monitoring Longterm shoreline changes along Tamil Nadu, India Using Geospatial Techniques. Aquat Procedia, 4, 325–332. https://doi.org/10.1016/j.aqpro.2015.02.044.

Phai V.V (editor), 2013. Studying and assessing coastal changes in Southern provinces (Vietnam) under the impact of climate change and sea level rise; Project code BĐKH.07, Hanoi (in Vietnamese).

Pilkey O.H., Hume T.M., 2001. The shoreline erosion problem: lessons from the past. Water Atmos., 9, 22–23.

Samanta S., Paul S.K., 2016. Geospatial analysis of shoreline and land use/ land cover changes through remote sensing and GIS techniques. Model Earth Syst Environ., 2, 108–108. https://doi.org/10.1007/s40808-016-0180-0.

Son H.T., Anh T.V., 2019. Determination of drainage corridor in the downstream Vu Gia - Han river, Da Nang city. Vietnam Joumal of Earth Sciences, 41(1), 46–58, https://doi.org/10.15625/0866-7187/41/1/13546.

Thai T.H., Tri D.Q., 2019. Combination of hydrologic and hydraulic modeling on flood and inundation waming: case study at Tra Khuc-Ve River basin in Vietnam. Vietnam Joumal of Earth Sciences, 41(3), 240–251. https://doi.org/10.15625/0866-7187/41/3/13866.

Thai T.H., Tri D.Q., Hoang D.V., 2018. Research on The Affected Simulation of Waves and Storm Surge In Coastal Central Vietnam. Vietnam Journal of Hydrometeorology, 03/2018, 1–14 (in Vietnamese with English abstract).

Thoai D.T., Dang A.N., Oanh N.T.K., 2019. Analysis of coastline change in relation to meteorological conditions and human activities in Ca Mau cape, Viet Nam. Ocean Coast Manag., 171, 56–65. https://doi.org/10.1016/j.ocecoaman.2019.01.007.

Thuy N.N (editor), 1995. East Sea tides and sea level rise on coastal zone of Vietnam, Project code KT.03.03, Hanoi, 199p (in Vietnamese).

Tung T., 2011. Morphodynamics of Seasonal Closed Coastal Inlets at the Central Coast of Vietnam, s.l.: Ph.D. Thesis. Delft University of Technology, 191p.

Turner I.L., Harley M.D., Short A.D., Simmons J.A., Bracs M.A., Phillips M.S., Splinter K.D., 2016. A multi-decade dataset of monthly beach profile surveys and inshore wave forcing at Narrabeen, Australia. Sci. Data, 3, 160024.

UNEP, 2008. Protocol on Integrated Coastal Zone Management in the Mediterranean.

UNEP/GPA, 2009. Annotated guiding principles for post-tsunami rehabilitation and reconstruction. United Nations Environment Programme Tsunami Disaster Task Force in cooperation with the UNEP Coordination Office of the Global Programme of Action for the Protection of the Marine Environment from Land-based Activities. Cairo.

Van N.K., Thuy D.L., Duc T.A., 2013. Causes and occurring frequency of heavy rain, “unusual heavy rain” in the area from Hai Van Pass to Ca Pass, South - Central Region of Vietnam (period 1986-2010). Journal of Sciences of the Earth, 35(2), 163–174 (in Vietnamese with English abstract).

VNA (Vietnam’s National Assembly), 2015. Law on natural resources and environment of sea and islands. No.82/2015/QH13 (In Vietnamese).

Wicaksono A.I., Wicaksono P., Khakhim N., Farda N.M., Marfai M.A., 2018. Tidal Correction Effects Analysis on Shoreline Mapping in Jepara Regency. JAGI. 2 (2/2018), 145–151. https://doi.org/10.30871/jagi.v2i2.981.

Williams A.T., Rangel-Buitrago N., Pranzini E., Anfuso G., 2018. The management of coastal erosion. Ocean Coast Manag., 156, 4–20. https://doi.org/10.1016/j.ocecoaman.2017.03.022.

Xu D., Guo X., 2014. Compare NDVI extracted from Landsat 8 imagery with that from Landsat 7 imagery. Am J. Remote Sens., 2, 10–14.

Xu H, 2006. Modification of normalised difference water index (NDWI) to enhance open water features in remotely sensed imagery. International Journal of Remote Sensing., 27(14), 3025–3033.